

A Multi-Junction Photodetector with Dual Four Transistor Structure to Detect Visible and Near-infrared Light in One Single Pixel.

Weihan Hu¹ and Albert J. P. Theuwissen^{1,2}

1. Electronic Instrumentation Laboratory, Delft University of Technology, Delft 2628CD, The Netherlands

2. Harvest Imaging, Bree, 3960, Belgium

Abstract—In this paper, we discuss a new type of CMOS image sensor (CIS) pixel which can separately detect visible and near-infrared (NIR) light in one single pixel by collecting the electrons and holes generated respectively. In the pixel design, an n-type and p-type four-transistor (4-T) pinned photodiode (PPD) are stacked back-to-back. The shallower located n-type 4-T PPD can collect electrons generated by visible light, while the deeper p-type 4-T PPD is applied for holes collection, mainly generated by NIR light. The special structure is designed, simulated and will be fabricated with an n-type substrate in a standard 0.18 μm CIS technology. Compared to a standard 4-T PPD pixel, only four extra photomasks and five extra implants are applied. The area of the prototype pixel is 17*17 μm^2 .

Keywords – Stacked photodiodes, visible light and NIR light sensing, CMOS image sensor (CIS), pixels, electrons and holes collection.

I. Introduction

In a semiconductor photodiode, incident photons absorbed by the silicon can generate electron-hole pairs. Theoretically, the photon-generated electrons and holes contain identical information of the input signal. In other words, we only need to collect one charge-carrier type. Considering the charge-mobility difference between electrons and holes [1], electrons are selected in most cases. Although under a proper operation, holes play a very broad role to improve the image quality [2], the excess holes are normally treated as a by-product. Taking an n-type 4-T PPD pixel as an example, the holes are drained directly to the ground through the low-resistivity path of the non-depleted p+ pinning-layer and p-type substrate.

However, in our design, the hole role is expanded. We are aiming at combining the sensing of visible light and near-infrared (NIR) light together by collecting electrons (visible light generated) and holes (NIR light generated) in one single pixel. Figure 1 shows a cross-section of the simplified pixel structure

considered in this work. Along the AA' line, from the surface to the substrate, it is firstly the p+ pinning-layer, the n-well for electrons collection, the p-well for holes collection and the n-type substrate. As a result, this structure has three p-n junctions ($p^+-n_{\text{well}}-p_{\text{well}}-n_{\text{sub}}$) stacked together, so we call it a multi-junction photodetector (MJPD).

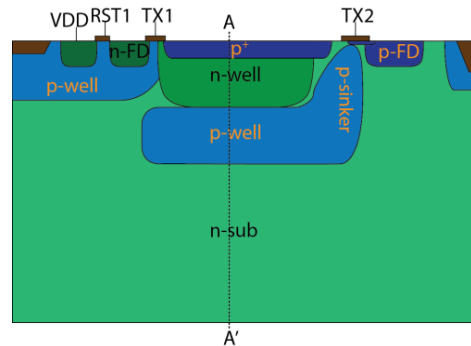


Figure 1 MJPD Dual 4-T PPD structure

In Figure 1, the visible light-generated electrons are collected in the n-well and then transferred to the n-type floating-diffusion (n-FD) node through the n-type transfer-gate (TX1). The NIR light has a longer wavelength and experiences a lower absorption coefficient [3], which makes the electron-hole generation location deeper in the silicon than that of the visible light. The generated holes are collected in the deeper p-well and transferred to the p-type FD (p-FD) node through a p-type transfer-gate (TX2). In order to smoothen and fasten the holes transfer, a p-type sinker is built to provide a vertical electrical field from the p-well to the surface. A buried channel beneath TX2 is also applied to help the holes further overcome the potential barrier along the path to the p-FD. The three stacked p-n junctions and the two separated FD nodes make the MJPD pixel a stacked dual 4-T PPD structure. In order to achieve this structure, there are three basic conditions to meet.

II. Three Basic Conditions

In the vertical direction, the stacked $p^+n\text{-well}p\text{-well}n\text{-sub}$ structure of MJPD is quite similar to the structure of a vertical overflow drain (VOD) in CCDs [4][5]. However, unlike an anti-blooming charge transferring path, this dual 4-T structure has to collect and transfer the photon-generated free charges, which makes this design much more complicated. In order to guarantee a proper charge collection and transfer performance, there are three basic conditions to be satisfied:

- a. For photon absorption, it requires proper $p\text{-}n$ junction depths for both visible and NIR light photons.

In our design, the junction depth for electrons collection is kept the same as a conventional 4-T PPD which is around $1.5\mu\text{m}$. For NIR light, the deeper $p\text{-}n$ junction depth is located around $4\mu\text{m}$. [6]

- b. For charge carriers generation and collection, it requires the photon sensing region to be fully depleted.

The application of a fully depleted n-well is one of the most important improvement of the CIS design. It has so many advantages, such as the elimination of image lag [7], the suppression of dark current [8] [9], a fixed build-in potential [10], and the possibility to apply correlated double sampling [11]. In order to take all these benefits in our design, a fully depleted n-well and a fully depleted p-well have become one of the three basic conditions.

- c. For charge carrier storage, the stacked n-well and p-well need to have a sufficient potential difference.

Figure 2 shows a simplified cross section and a one-dimensional potential distribution of the MJPD structure. The pinning layer is connected to the ground potential and the n-type substrate is biased at 6V .

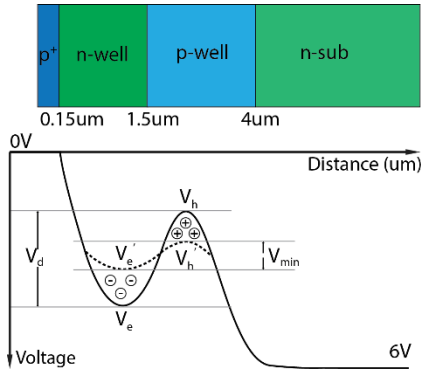


Figure 2 MJPD potential distribution

With proper implants, the n-well and p-well can become fully depleted, which will generate two fixed

pinning voltages V_e and V_h . V_d and V_{\min} stand for the potential difference and its minimum value between V_e and V_h , respectively.

As shown in Figure 2, during the illumination and charge collection procedure, V_e will decrease to V_e' with the accumulation of electrons; oppositely, V_h will increase to V_h' due to the collection of holes. In other words, this charge collection procedure will straighten up the potential curve of the stacked $p\text{-}n$ junctions. Considering the charge emission theory [12], the potential difference after charge collection should be larger than 1V to ensure the storage of the collected electrons and holes for long enough time without compensation.

III. TCAD Simulations

For our design, the TCAD simulation includes mainly two parts: the process and device simulations. The process simulation defines the process flow and the photomasks design for the silicon fabrication. Based on that, a device simulation can be applied, so as to check the MJPD mechanisms.

In our design, the process simulation starts with a standard 4-T PPD layout and follows its actual fabrication steps. With four extra photomasks and five extra implants, the MJPD structure is achieved. Figure 3 shows the doping concentration map of the MJPD pixel. The dopant atoms distribution are marked with color spectra. Acceptors are more to the blue color side and donors are more to the red color side. As can be seen, the starting materials is n-type silicon. The four extra photomasks are applied for the implantations of the deeper p-well (DPW), the p-type sinker (SNK), the buried channel beneath TX2 and an anti-leakage n-type doping between the sinker and p-FD. The junction depth of deeper p-well is located around $4\mu\text{m}$, which meets the requirement of the first basic condition for NIR light collection.

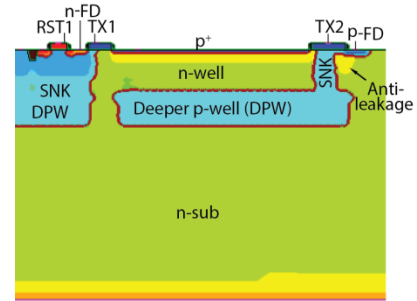
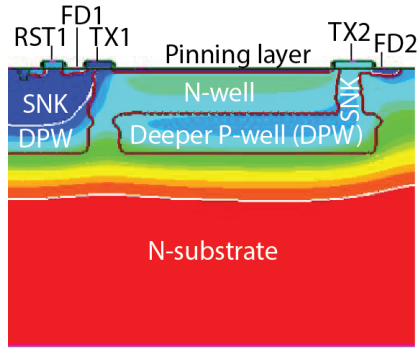


Figure 3. A doping concentration map of the MJPD structure.

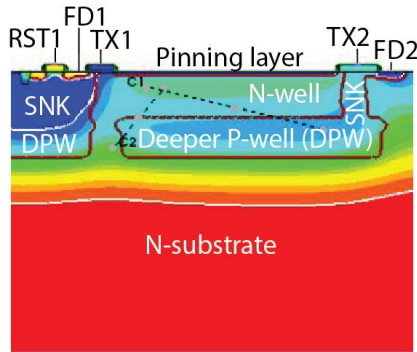
After the device simulation, the potential distribution results are shown in Figure 4. Figure 4 (a) shows the state just after the reset of both photodiodes, there are no free charges (no white contour circles) located in the n-well and p-well, which means both the

n-well and p-well can be fully depleted under specific bias conditions. As a result, the white contours in both the n & p-well region, in Figure 4 (b), are charges that are generated by an illumination process and then transferred out in the following Figure 4 (c).

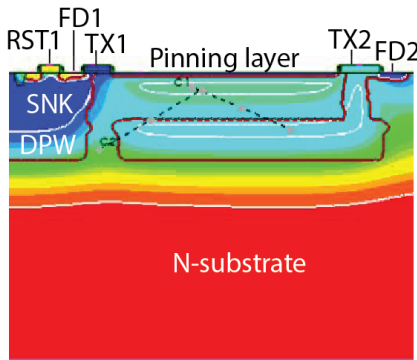
In Figure 4 (b) and Figure 4 (c), two critical potential gradients are marked by two dashed lines. Line AB demonstrates the maximum potential difference V_{AB} between the centers of the n-well and p-well. As shown in Figure 4 (d), the curves in red and blue colors stand for the potential V_{AB} , which are 1V and 1.4V with or without charge collection, respectively.



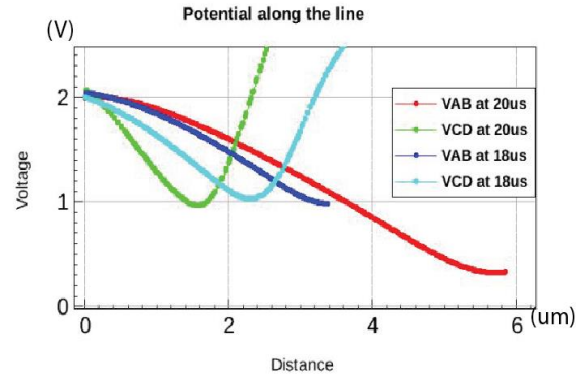
(a)



(b)



(c)



(d)

Figure 4 Results of TCAD device simulations showing the potential distribution map of the MJPD, (a) at $3\mu\text{s}$ simulation time (just after reset), (b) at $18\mu\text{s}$ (just after the illumination), (c) at $20\mu\text{s}$ after the charge transfer, (d) the potential distribution along line AB and CD.

The line CD goes through the saddle point generated between the two p-well regions, which illustrates the potential barrier V_{CD} along this possible electron leakage path. As the two curves (in cyan and green colors) in Figure 4 (d) shown, V_{CD} is always larger than 1V. As a consequence, our third basic condition, which requires sufficient potential barrier to hold the charges, is satisfied as well.

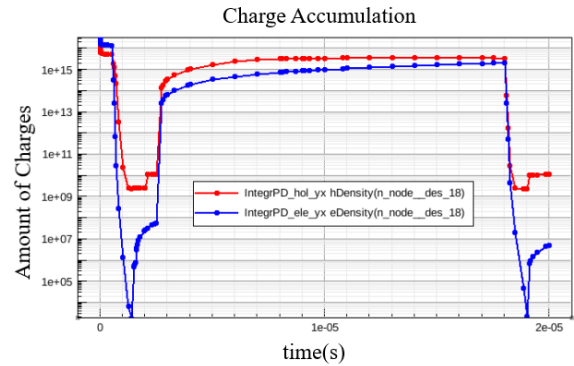


Figure 5 Charge Accumulation Results. The red curve stands for hole density and the blue curve stands for electron density.

In the device simulation conditions, the “optical beam absorption” method was applied for the optical generation. The incident photons have a wavelength of 800nm, an intensity of $7\text{mW}/\text{cm}^2$ and an illumination time of $15\mu\text{s}$ focusing on the active area between the two transfer-gates. The charge accumulation results are shown in Figure 5. The red curve stands for hole density and the blue curve stands for electron density. As can be seen, both curves show a significant drop at $2\mu\text{s}$, due to the reset phase; the charge amounts start to increase at $2.5\mu\text{s}$ until $17.5\mu\text{s}$, just before the charge transfer starts. As a result, not only our second

condition about fully depletion, but also the charge generation and transfer mechanisms are proven.

IV. Conclusion

This work proves the possibility of combining the detection of the visible and NIR light together in one single pixel, by collecting electrons and hole with a stacked dual 4-T PPD multi-junction photodetector structure. We explained the three basic conditions in order to achieve this MJPD structure. In the simulation work, the entire mechanisms of the MJPD, including the three basic conditions and the functions like optical generation and charge transferring are proven. Compared to a standard 4-T PPD, the MJPD structure is achieved with four extra photomasks and five more times implants. All the changes are compatible to the standard CMOS image sensor technology. The area of the prototype pixel is $17 \times 17 \mu\text{m}^2$. The measurement results and specific performance of the device will be included in following publications.

Acknowledgement

The authors would like to thank NWO Domain Applied and Engineering Sciences (TTW), Prof. Alexander Fish, Erez Tadmor and other colleagues from Bar-Ilan university and the foundry Tower Jazz, for their generous help with designing and prototyping the test-chips.

References

- [1] M. Grundmann, *Physics of semiconductors* vol. 11, pp. 191-193: Springer, 2010.
- [2] A. J. P. Theuwissen, "The Hole Role in Solid-State Imagers," *IEEE transactions on Electron Devices*, vol. 53, pp. 2972-2980, 2006.
- [3] S. M. Sze and K. K. Ng, *Physics of semiconductor devices*, pp. 51-52: John wiley & sons, 2006.
- [4] A. J. Theuwissen, *Solid-state imaging with charge-coupled devices* vol. 1, pp. 179-182: Springer Science & Business Media, 2006.
- [5] S. Ochi, T. Lizuka, M. Hamasaki, Y. Sato, T. Narabu, H. Abe, et al., *Charge-coupled device technology* vol. 30, pp. 20-25: CRC Press, 1997.
- [6] E. Tadmor, A. Lahav, A. Fish, G. Yahav, and D. Cohen, "A high QE, fast shuttered CMOS image sensor with a vertical overflow drain shutter mechanism," in *Proc. Int. Image Sensor Workshop*, 2015.
- [7] N. Teranishi, A. Kohono, Y. Ishihara, E. Oda, and K. Arai, "No image lag photodiode structure in the interline CCD image sensor," in *1982 International Electron Devices Meeting*, 1982, pp. 324-327.
- [8] B. Mheen, Y.-J. Song, and A. J. Theuwissen, "Negative offset operation of four-transistor CMOS image pixels for increased well capacity and suppressed dark current," *IEEE electron device letters*, vol. 29, pp. 347-349, 2008.

- [9] A. Dokoutchaev, B. Gravelle, H. L. W. Qian, and R. Johnson, "Pixel continues to shrink.... Small Pixels for Novel CMOS Image Sensors," in *Proc. Int. Image Sensor Workshop*, 2011.
- [10] J. Hynecsek, "Virtual phase CCD technology," in *1979 International Electron Devices Meeting*, 1979, pp. 611-614.
- [11] M. White, D. Lampe, I. Mack, and F. Blaha, "Characterization of charge-coupled device line and area-array imaging at low light levels," in *1973 IEEE International Solid-State Circuits Conference. Digest of Technical Papers*, 1973, pp. 134-135.
- [12] E. R. Fossum, "Charge transfer noise and lag in CMOS active pixel sensors," in *Proc. 2003 IEEE Workshop on CCDs and Advanced Image Sensors, Elmau, Bavaria, Germany*, 2003, pp. 11-13.